ANTICANCER RESEARCH *37*: 4779-4788 (2017)
doi:10.21873/anticanres.11884

Gefitinib Enhances Mitochondrial Biological Functions in NSCLCs with *EGFR* Mutations at a High Cell Density

TOMOYA TAKENAKA[1,2], MIKU KATAYAMA[1,2], AYAKA SUGIYAMA[1,2], MASAYA HAGIWARA[1], IKUO FUJII[2], TOMOKA TAKATANI-NAKASE[3], SUSUMU S. KOBAYASHI[4] and IKUHIKO NAKASE[1]

[1]*NanoSquare Research Institution, Research Center for the 21st Century, Organization for Research Promotion, Osaka Prefecture University, Sakai, Japan;*
[2]*Graduate School of Science, Osaka Prefecture University, Osaka, Japan;*
[3]*Department of Pharmaceutics, School of Pharmacy and Pharmaceutical Sciences, Mukogawa Women's University, Nishinomiya, Japan;*
[4]*Beth Israel Deaconess Medical Center, Harvard Medical School, Boston, MA, U.S.A.*

Abstract. *Background/Aim: Gefitinib is a tyrosine kinase inhibitor of epidermal growth factor receptor (EGFR) and has been approved for the treatment of non-small cell lung cancers (NSCLCs) with EGFR mutations. Here we demonstrated that gefitinib induced a significantly enhanced biological activity of succinate-tetrazolium reductase (STR) in mitochondria and mitochondrial membrane potential in HCC827 cells (EGFR mutation NSCLCs, sensitive to gefitinib) at a high cell density. Materials and Methods: We assessed the biological activity (STR, mitochondrial membrane potential, expression level of Bcl-2 family proteins) of gefitinib on NSCLCs at different cell densities. Results: The 3D cell culture experiments showed the enhanced mitochondrial biological activity in clustered cell culture treated with gefitinib. Interestingly, the expression levels of Bcl-x_L and Bax, were affected by the cellular number and gefitinib treatment. We also found that gefitinib prevented additive anticancer activity in the combinational treatment with doxorubicin, which induces mitochondria-dependent apoptotic cell death. Conclusion: Our results indicate that gefitinib may work as a mitochondrial protector against combinational treatment with mitochondria-dependent anticancer agents in high-cell-density.*

Correspondence to: Susumu S. Kobayashi, Beth Israel Deaconess Medical Center, Harvard Medical School, Boston, MA 02215, U.S.A. Tel: +1 6177352229, Fax: +1 6177352222, e-mail: skobayas@bidmc.harvard.edu; Ikuhiko Nakase, NanoSquare Research Institution, Research Center for the 21st Century, Organization for Research Promotion, Osaka Prefecture University, 1-2, Gakuen cho, Naka-ku, Sakai, Osaka 599-8570, Japan. Tel: +81 722549895, Fax: +81 722549895, e-mail: i-nakase@21c.osakafu-u.ac.jp

Key Words: Gefitinib, non-small cell lung cancer, mitochondria, EGFR, anti-cancer activity.

Gefitinib [N-(3-chloro-4-fluoro-phenyl)-7-methoxy-6-(3-morpholin-4-ylpropoxy) quinazolin-4-amine, commercial name: Iressa] (Figure 1A) is a tyrosine kinase inhibitor (TKI) for epidermal growth factor receptor (EGFR) and has been approved for the treatment of non-small cell lung cancers (NSCLCs) with *EGFR* mutations (1-6). Patients with a sensitizing exon 19 deletion or an exon 21 substitution mutation of *EGFR* are highly responsive to gefitinib (7). EGFR phosphorylation triggers intracellular signaling cascades including Ras-receptor accessory factor (RAF)-mitogen-activated protein kinase (MAPK), phosphatidyl inositol 3-kinase (PI3K)-Akt, and JAK-STAT pathways, all of which are involved in the process of cellular proliferation, anti-apoptosis, angiogenesis activation, and cancer metastasis (8). Overexpression of EGFR observed in breast cancer tissues is associated with aggressive metastatic breast tumors (9, 10). Activating mutations in the *EGFR* gene result in constitutive activation of EGFR and downstream signaling pathways leading to promotion of cancer growth and metastasis (7, 11). Gefitinib selectively binds to the kinase domain and inhibits phosphorylation of EGFR, resulting in suppression of downstream signals leading to apoptotic cell death (2, 3, 7, 12-19). Despite its dramatic effects, resistance to gefitinib develops within 1 or 2 years. In addition, prolonged exposure to gefitinib induces resistance against anticancer drugs (20). However, the mechanisms of these effects are still unclear.

In this study, we assessed the biological activity of gefitinib on NSCLC including HCC827 cells (an activating *EGFR* mutation [del E746-A750]), that are sensitive to gefitinib, and A549 cells (expression of wildtype EGFR), that are resistant to gefitinib. We found that gefitinib significantly enhanced enzymic activity of mitochondrial

respiratory chain enzyme succinate-tetrazolium reductase (STR) and mitochondrial membrane potential in HCC827 cells under a high cell density condition. The expression levels of Bcl-2 family proteins, Bcl-x_L and Bax, were affected by the cell number and gefitinib treatment. Interestingly, a combination of gefitinib and doxorubicin, which induces mitochondria-mediated apoptotic cell death, did not show an additive effect. Our results suggest that cell density-dependent regulation of mitochondrial membrane potential may lead to emergence of resistance to EGFR-TKIs and other treatments.

Materials and Methods

Materials. Gefitinib (Cell Signaling Technology, Inc., Danvers, MA, USA), human epidermal growth factor (EGF) and penicillin-streptomycin (Sigma-Aldrich Co., Inc., St. Louis, MO, USA), RPMI1640 and fetal bovine serum (FBS) (Gibco, Life Technologies Corporation, Grand Island, NY, USA), Dulbecco's phosphate buffered saline (PBS) and trypsin (0.5 g/l) /ethylenediaminetetraacetic acid (EDTA) (0.53 mmol/l) solution with phenol red (Nacalai Tesquen Inc., Kyoto, Japan), dimethyl sulfoxide (DMSO), and doxorubicin (Wako Pure Chemical Co., Inc., Osaka, Japan), Premix WST-1 (4-[3-(4-iodophenyl)-2-(4-nitrophenyl)-2H-5-tetrazolio]-1,3-benzene disulfonate) cell proliferation assay system (Takara Bio Inc., Shiga, Japan), JC-1 (5, 5', 6, 6'-tetrachloro-1, 1', 3, 3'-tetraethylbenzimida-zolylcarbocyanine iodide) (Setareh Biotech, LLC., Eugene, OR, USA) were purchased.

Cell culture. Two NSCLCs, HCC827 and A549 (the American Type Culture Collection, Manassas, VA, USA) were cultured in RPMI 1640 containing 10% FBS on 100-mm dishes (Iwaki, Tokyo, Japan) and incubated at 37˚C under 5% CO_2.

WST-1 assay. HCC827 or A549 cells (3.0×10^3 or 1.2×10^4 cells/well (100 μl/well)) were incubated in 96-well microplates (Iwaki) for 24 h at 37˚C. After removal of the medium, the cells were then treated with each experimental sample (50 μl/well) containing epidermal growth factor (EGF, 10 nM) and penicillin (100 units/ml)-streptomycin (0.1 mg/ml) for 72 h at 37˚C. After the sample treatment, Premix WST-1 reagent (10 μl) was added to each well, and the samples were incubated for 45 min at 37˚C. Absorbance was measured at 450 nm (A450) and 620 nm (A620), and the value obtained by subtracting A620 from A450 corresponded to activation of STR.

Cell viability (living cell counting). HCC827 or A549 cells (each 1.2×10^4 cells/well (100 μl/well)) were incubated in 96-well microplates for 24 h at 37˚C. After removal of medium, the cells were then treated with each experimental sample (50 μl/well) containing EGF (10 nM) and penicillin (100 units/ml)-streptomycin (0.1 mg/ml) for 72 h at 37˚C. After the sample treatment, the cells were washed with PBS (triple washing, 50 μl) and treated with trypsin (0.1 g/l)-EDTA (0.11 mmol/l) (50 μl/well) at 37˚C for 10 min. Following the addition of RPMI1640 medium (50 μl), the suspension cells were centrifuged at 1,500 rpm (200 × *g*) for 5 min at 4˚C. After removal of supernatant solution, the cells were added with RPMI1640 medium (100 μl) and then the living cell number was counted using OneCell Counter (Bio Medical Science Inc. Tokyo, Japan).

Confocal microscopy. HCC827 or A549 cells (each 3.6×10^5 cells/well (3 ml)) were plated on 35-mm glass-based dishes (Iwaki) and incubated for 24 h at 37˚C. After removal of the medium, the cells were then treated with each experimental sample (1.5 ml/well) containing EGF (10 nM) and penicillin (100 units/ml)-streptomycin (0.1 mg/ml) for 72 h at 37˚C. After the sample treatment, the medium was removed and the cells were treated with JC-1 (10 μM, 100 μl) at 37˚C for 20 min. The cells were then washed with fresh cell culture medium (three times, 1 ml) and analyzed using a FV1200 confocal laser scanning microscope (Olympus, Tokyo, Japan).

Flow cytometry. HCC827 or A549 cells (7.2×10^4 cells, 1 ml) were plated on a 24-well microplate (Iwaki) and incubated for 24 h at 37˚C. After removal of medium, the cells were then treated with each experimental sample (300 μl/well) containing EGF (10 nM) and penicillin (100 units/mL)-streptomycin (0.1 mg/mL) for 72 h at 37˚C. After the sample treatment, the cells were washed with PBS (triple washing, 200 μl) and treated with trypsin (0.1 g/L)-EDTA (0.11 mmol/L) (200 μl/well) at 37˚C for 10 min. Following the addition of RPMI1640 medium (200 μL), the suspension cells were centrifuged at 1,500 rpm for 5 min at 4˚C. After removal of supernatant solution, the cells were treated with JC-1 (10 μM, 400 μl) at 37˚C for 20 min and subjected to fluorescence analysis on a Guava EasyCyte (Merck Millipore, Billerica, MA, USA) flow cytometer using 488 nm laser excitation and a 525 nm (monomer) or 583 nm (J-aggregation) emission filter.

3D-cell clustering assay. Matrigel was used to develop 3D clustering cells. To mimic the 2D cell-culturing conditions with different cell concentrations, same number of the HCC827 or A549 cells were dispersed homogeneously in Matrigel to mimic the low cell concentration condition or injected in the center of Matrigel at a point to mimic the high cell concentration condition. After the HCC827 or A549 cells (1.5×10^5 cells in 20 μl Matrigel) were incubated in 96-well microplates for 25 min at 37˚C to form hydrogel, cells were treated with 200 μL medium and incubated for 24 h at 37˚C. After removal of the medium, the cells were then treated with cell culture medium (200 μL) containing EGF (10 nM), penicillin-streptomycin (100 units/ml and 0.1 mg/ml), and gefitinib in each experimental concentration for 72 h at 37˚C. After the sample treatment, Premix WST-1 reagent (10 μl) was added to each well, and the samples were incubated for 45 min at 37˚C. Absorbance was measured at 450 nm (A450) and 620 nm (A620), and the value obtained by subtracting A620 from A450.

Western blotting analysis. HCC827 or A549 cells (7.2×10^4 or 1.8×10^4 cells, 1 ml) were treated with each experimental sample (300 μl/well) containing EGF (10 nM) and penicillin (100 units/ml)-streptomycin (0.1 mg/mL) for 72 h at 37˚C. After the sample treatment, the cells were scraped in lysis buffer (200 μl). The boiled lysate samples were separated by 10% SDS-PAGE, then transferred to PVDF membranes (GE Healthcare, Pittsburgh, PA, USA), and treated with Bax antibody (2774, Cell Signaling Technology, Danvers, MA, USA), Bcl-x_L antibody (sc-1041, Santa Cruz Biotechnology, Santa Cruz, CA), E-cadherin antibody (610181, BD Biosciences, Franklin Lakes, NJ, USA), β-actin (A1978, Sigma-Aldrich, St. Louis, MO, USA). Secondary antibody labeled with horseradish peroxidase (anti-rabbit IgG HRP-linked whole antibody donkey, or anti-mouse IgG HRP-linked whole antibody, GE Healthcare, Pittsburgh, PA, USA) was then used, and

immunoreactive species were detected by ECL Plus Western Blotting Detection System (GE Healthcare) with the Amersham Imager 600 (GE Healthcare, Pittsburgh, PA, USA). The band intensities were analyzed by ImageJ software.

Statistical analyses. All statistical analyses were performed using GraphPad Prism software (ver. 5.00; GraphPad, San Diego, CA, USA). For comparisons of two groups, unpaired Student's *t*-test was used for verification of the equal variances *via* an F-test. Welch's correction was performed when the variances across groups were assumed to be unequal. For multiple comparison analyses, a one-way analysis of variance (ANOVA) followed by Dunnett's or Tukey's multiple comparison test was used. Differences were considered significant when the calculated *p*-value was <0.05.

Results

Activation of mitochondrial STR by treatment of gefitinib. HCC827 is one of NSCLC cell lines with an activating EGFR mutation (del E746-A750), and sensitive to gefitinib, whereas A549 harbors wildtype EGFR and is resistant to gefitinib. Cells were treated with gefitinib for 72 h prior to analysis of WST-1 assay, which detects activation of STR (Figure 1B) (21). Gefitinib (30 nM~10 μM) induced a significant increase in absorbance for detection of STR in HCC827 cells when they were plated at high density (12,000 cells/well) (Figure 1D), whereas a decrease in absorbance was observed at low density (3,000 cells/well) (Figure 1C). However, gefitinib induced very slight absorbance changes in A549 cells (Figure 1E).

Formation of HCC827 cell cluster increases biological activity of STR by gefitinib. Our findings that a high cell density led to an increase in biological STR activity (Figure 1D) prompted us to assess effects of gefitinib on cell cluster formation using the 3D cell culture experiment. HCC827 and A549 cells were plated on cell culture plates in the formation of dispersed cells (Figure 2A and E) or cell cluster (Figure 2C and G). After the gefitinib treatment for 72 h, WST-1 assay was done in each cell. In the case of HCC827 cell cluster formation, STR activity was similar to that of control (no treatment) (Figure 2D), whereas very low biological activity of STR was detected in dispersed cell formation by gefitinib treatment (Figure 2B). On the other hand, in the case of A549 cells, each dispersed cell and cell cluster formation showed similar STR activity when the cells were treated with gefitinib (Figure 2F and H). These results suggest that cell density may affect biological activity of STR upon gefitinib treatment in gefitinib-sensitive NSCLCs.

Mitochondrial membrane potential is enhanced upon gefitinib treatment. Reduction of WST-1 reagent needs a proton donated from nicotinamide adenine dinucleotide (NADH) (Figure 1B) (22). NADH is also crucial for maintaining mitochondrial membrane potentials, which control biological functions of mitochondria such as electron transport, generation of ATP and apoptotic cell death (23). JC-1 is cytofluorometric, lipophilic and cationic dye (24). In healthy cells, JC-1 forms complexes detected as J-aggregates with increasing red fluorescent intensity, which reflects high mitochondrial membrane potential. On the other hand, JC-1 remains a monomeric form with green fluorescent intensity when mitochondrial membrane potential is low (24). When A549 cells were treated with gefitinib (10 nM) for 72 h, fluorescent intensity of JC-1 was not affected (Figure 3C). On the other hand, gefitinib significantly enhanced J-aggregates in mitochondria in HCC827 cells (Figure 3A and B). These results suggest that gefitinib induces an increase in mitochondrial membrane potential in *EGFR* mutated cells.

Gefitinib reduces anticancer biological activity of anti-cancer agents that induce apoptotic cell death via mitochondria. Next, we tested a combinational treatment of the anticancer reagent, doxorubicin, with gefitinib. An anthracycline antibiotic, doxorubicin, has been widely used for therapeutic cancer treatment (25-28). It has been shown that doxorubicin induces mitochondrial dysfunction and apoptotic cell death (28). When the cells were treated with doxorubicin (300 nM), morphological changes (rounded cells) were observed (Figure 4A). However, in the case of combinational treatment of doxorubicin with gefitinib, the morphological changes were scarcely observed (Figure 4A). Living cell counting analyses revealed that either gefitinib (100 nM) or doxorubicin alone (300 nM) inhibited cell growth in approximately half of the cells (Figure 4B). Despite this, a combination of gefitinib and doxorubicin did not demonstrate additive anti-cancer effects (Figure 4B). In the case of A549 cells, doxorubicin treatment significantly affected the cell growth in the presence or absence of gefitinib (Figure 4C).

Effects of cell numbers and gefitinib on expression levels of apoptosis-related proteins. Next, we examined the effects of cell numbers and gefitinib on the expression levels of apoptosis-related proteins by western blot analyses (Figure 5). High (72,000 cells/well) or low (18,000 cells/well) numbers of HCC827 or A549 cells were treated with gefitinib (0, 10, or 100 nM) for 72 h at 37˚C, prior to preparing cellular lysates and western blot analyses.

Bax is one of the pro-apoptotic Bcl-2 family members, and the oligomers of Bax are responsible for permeabilization of the mitochondrial outer membranes and cytochrome *c* release, leading to apoptotic cell death (29). On the other hand, Bcl-x_L is a pro-survival Bcl-2 family protein that inhibits proapoptotic activity of Bax/Bak (30, 31). As shown in Figure 5, in HCC827 cells, Bax expression was reduced and Bcl-x_L expression was increased at a higher cell density. On the other hand, in A549 cells, high

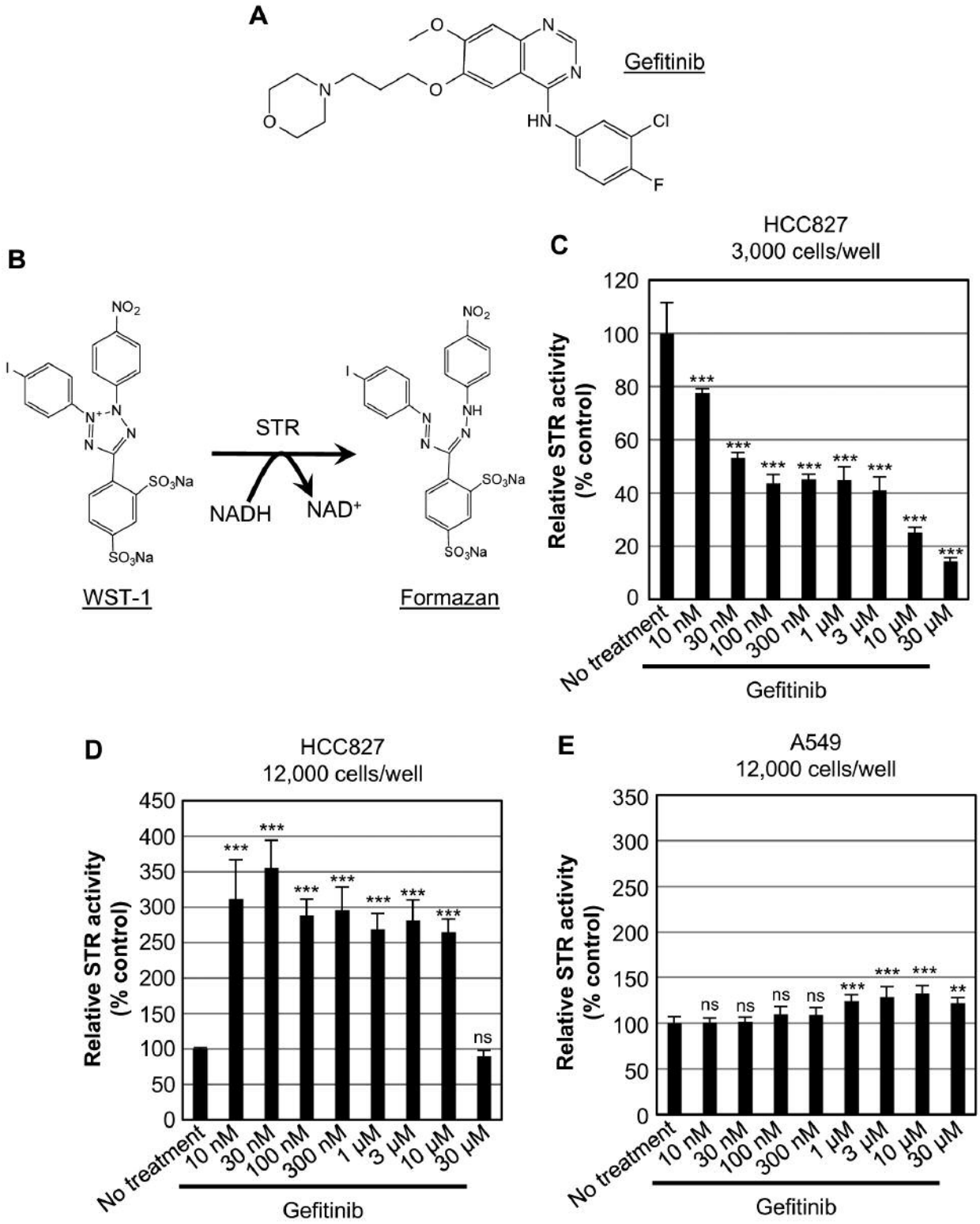

Figure 1. *Effects of gefitinib treatment on the biological activity of succinate-tetrazolium reductase. (A) Chemical structure of gefitinib. (B) Structure change of WST-1 by biological activity of succinate-tetrazolium reductase (STR). (C-E) WST-1 assay of HCC827 (3,000 cells/well: C, 12,000 cells/well: D) and A549 (12,000 cells/well: E) cells treated with gefitinib (0~30 μM) in 10% FBS-containing RPMI 1646 for 72 h at 37˚C to detect biological activity of succinate-tetrazolium reductase. The data are the averages (±SD) of four experiments. **p<0.01 between no treatment and each sample concentration. ***p<0.001 between no treatment and each sample concentration.*

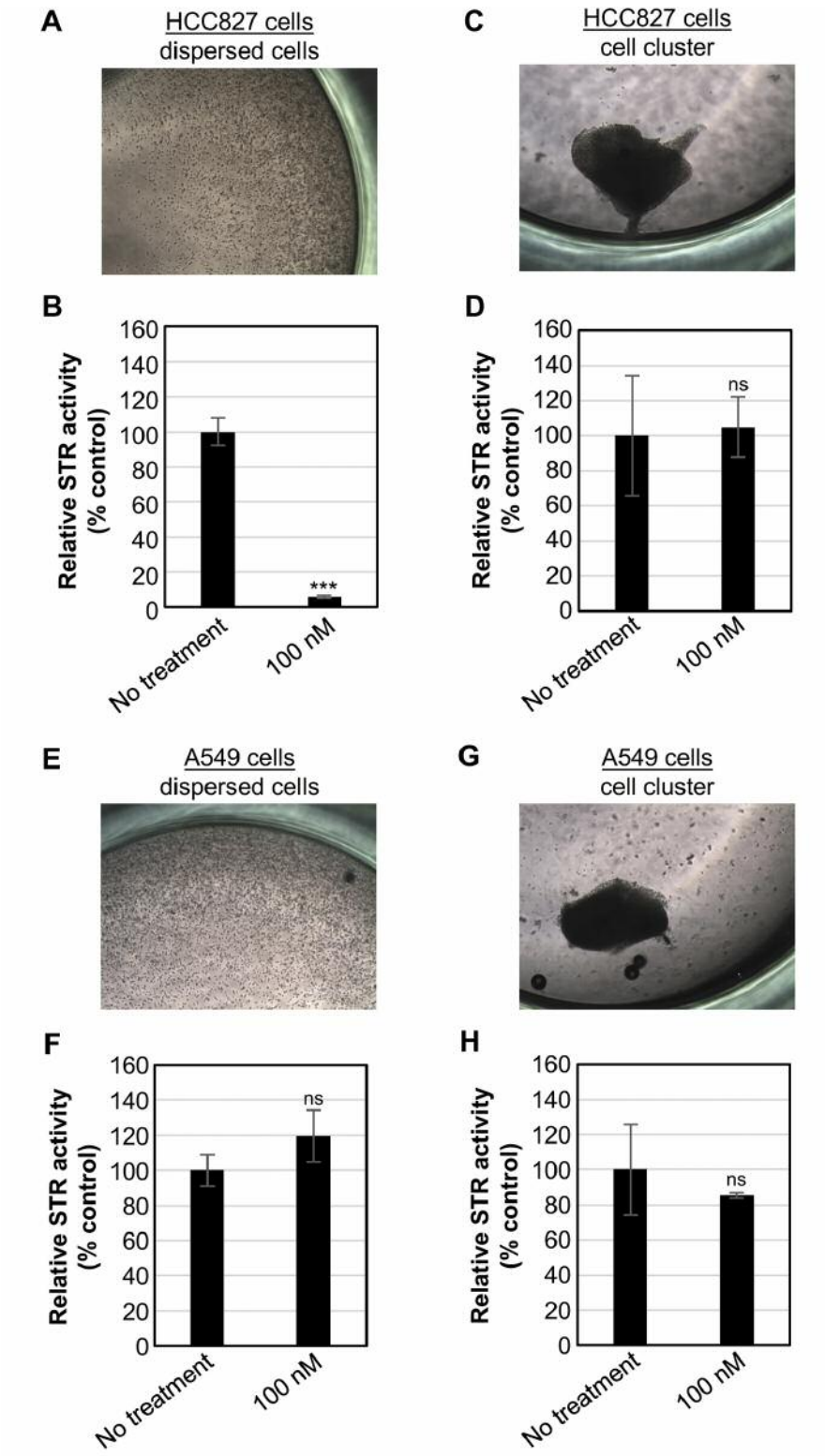

Figure 2. *Effects of cell cluster formation on biological activity of succinate-tetrazolium reductase by treatment of gefitinib. (A-D) HCC827 cells (dispersed cells (A), cell cluster (C)) were treated with or without gefitinib (100 nM) in 10% FBS-containing RPMI 1646 for 72 h at 37˚C, prior to WST-1 assay (dispersed cells (B), cell cluster (D)). (E-H) A549 cells (dispersed cells (E), cell cluster (G)) were treated with or without gefitinib (100 nM) in 10% FBS-containing RPMI 1646 for 72 h at 37˚C, prior to WST-1 assay (dispersed cells (F), cell cluster (H)). The data are the averages (±SD) of three experiments. ***p<0.001 between no treatment and each sample concentration.*

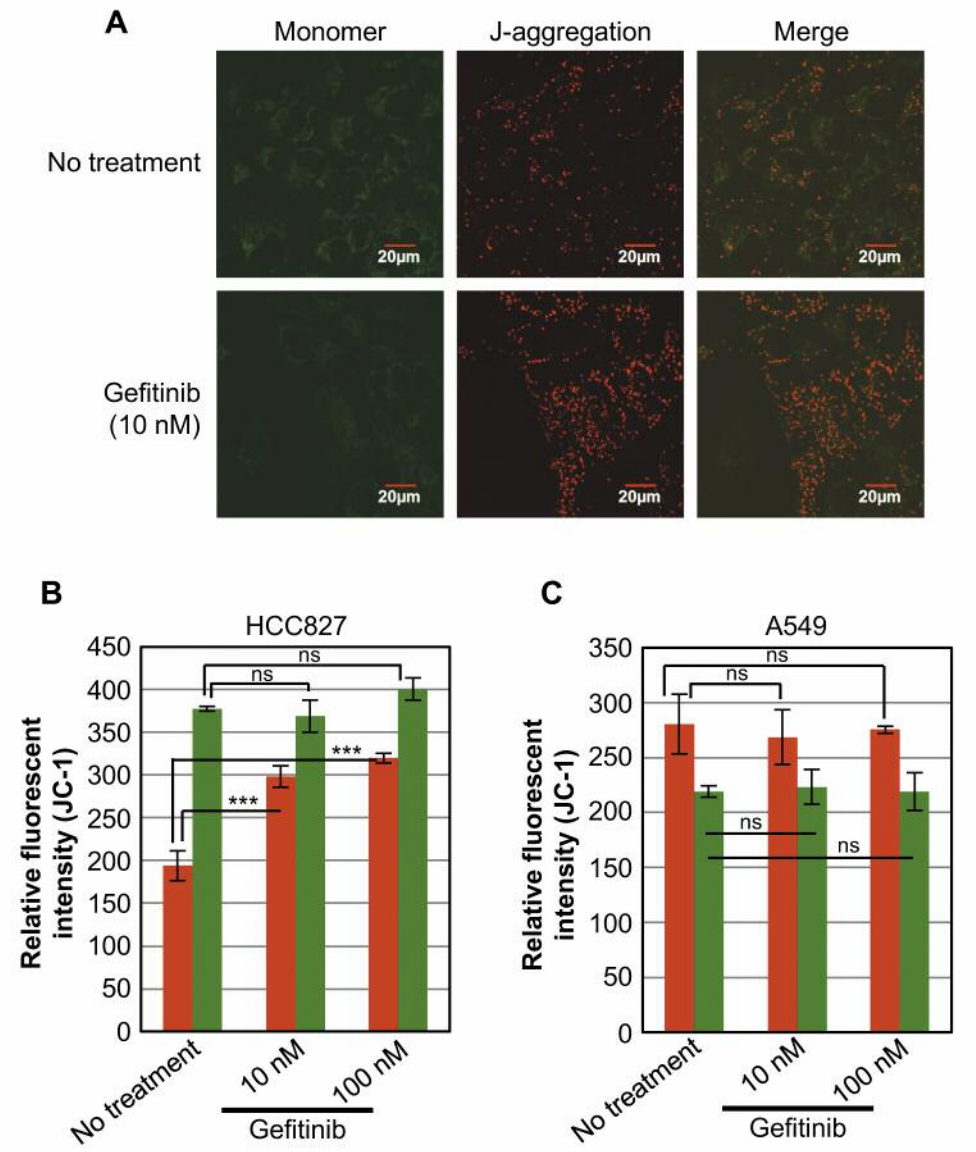

Figure 3. *Increased mitochondrial membrane potential by treatment of gefitinib on HCC827 cells. (A) Confocal microscopic observation of HCC827 cells treated with gefitinib (10 nM) in 10% FBS-containing RPMI 1646 for 72 h at 37˚C, prior to JC-1 staining to detect mitochondrial membrane potentials. Red: J-aggregates of JC-1 (responding to mitochondrial membrane potentials), green: monomer of JC-1. (B, C) Flow cytometric analysis of HCC827 (B) or A549 (C) cells treated in same experimental condition in (A). Red bars: J-aggregates of JC-1 (responding to mitochondrial membrane potentials), green bars: monomer of JC-1. The data are the averages (±SD) of three experiments. ***p<0.001.*

cell number of A549 oppositely increased expression of Bax. We calculated the expression ratio of Bcl-x_L/Bax to argue cellular survival ability, that might be related to resistance to other anticancer drugs. The ratio of Bcl-x_L/Bax in HCC827 cells under high density condition was almost twice as high as that under low density conditions regardless of gefitinib treatment.

In addition, we checked two expression levels of calcium-dependent cell-cell adhesion molecule, E-cadherin, which play crucial roles in tissue formation, and is suppressed on cancer cell membranes (32). In HCC827 cells, interestingly, E-cadherin expression level was decreased at a high density, that was not affected by gefitinib, suggesting that a high cell number of HCC827 might possibly enhance metastasis efficacy. On the other hand, in the case of A549 cells, E-cadherin expression level was rather increased at a high density, which was not affected by gefitinib treatment.

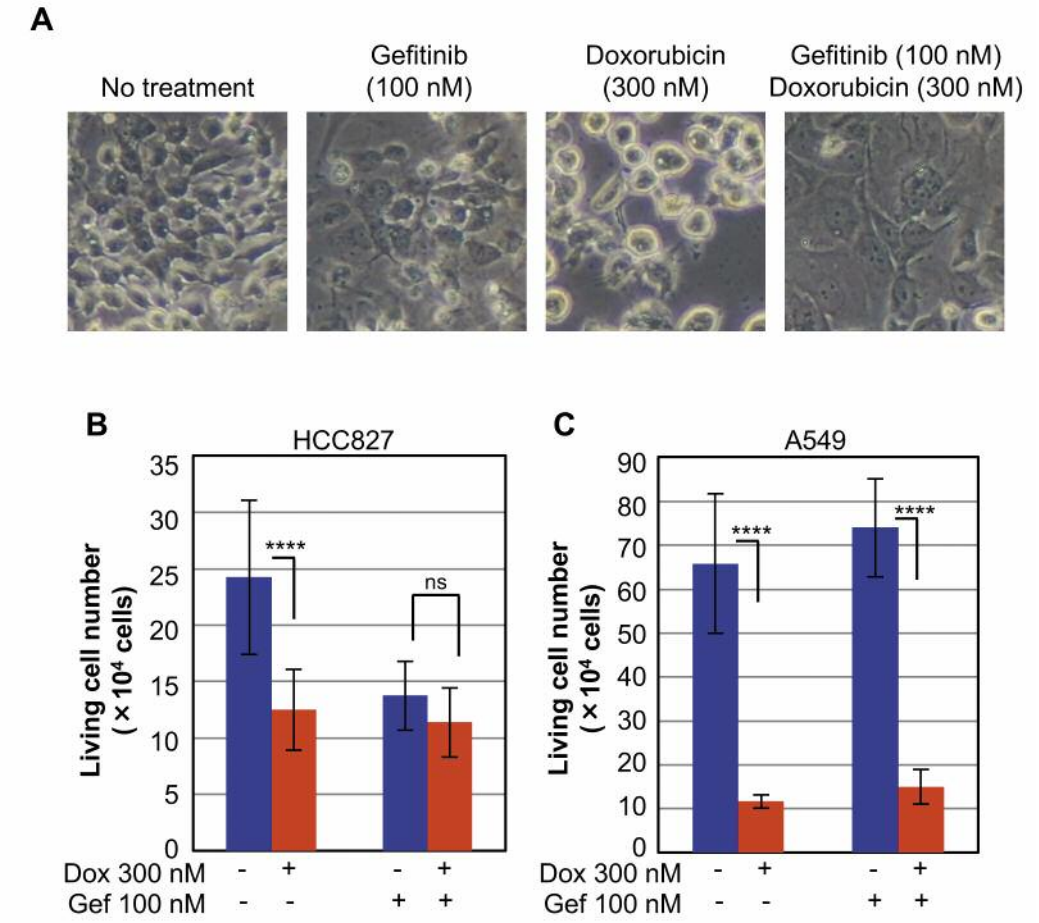

Figure 4. *Effects of gefitinib on combinational treatment with doxorubicin. (A) Microscopic observation of HCC827 cells treated with gefitinib (100 nM) or doxorubicin (Dox, 300 nM) in 10% FBS-containing RPMI 1646 for 72 h at 37˚C. (B, C) Living cell counting assay of HCC827 (B) or A549 (C) cells treated in same experimental condition in (A). The data are the averages (±SD) of eight experiments. ****p<0.0001.*

Discussion

In this research, we found that gefitinib enhances biological activity of STR and increases mitochondrial membrane potentials. Xia and Laterra reported that treatment of human glioblastoma cells with hepatocyte growth factor/scatter factor (HGF) followed by the topoisomerase inhibitor camptothecin increased the biological activity of STR (>80% increase, $p<0.05$) and the tricarboxylic acid cycle enzyme succinate dehydrogenase (>25% increase, $p<0.05$) (33). The authors concluded that HGF influences cell responses to chemotherapeutic stress by altering mitochondrial functions through a MAP-kinase dependent increase in mitochondrial mass (33). In our results, Figure 3A and B showed significantly increased JC-1 J-aggregate level in the HCC827 cells by gefitinib. Binding of gefitinib to the tyrosine kinase region of EGFR intracellular domain resulted in inhibition of downstream signals of the MAPK pathway (7, 14-18), and the molecular mechanisms in cellular responses to chemotherapeutic stress might be related to the case of HGF and topoisomerase inhibitor even though further elucidation should be needed. The mitochondrial permeability transition pore (MPTP) also plays a critical role to preserve the optimal mitochondrial membrane potential. Mitochondrial membrane permeability is increased by MPTP induction, leading to further depolarized, collapse of mitochondrial membrane potential, cytochrome *c* release from mitochondria to cytosol, mitochondrial swelling and cellular apoptosis (34, 35). Our results demonstrated that gefitinib led to an increased mitochondrial membrane potential in HCC827 cells at a high cell density suggesting that mitochondrial protection in this experimental condition possibly leads to resistance against mitochondria-mediated agents (Figures 3 and 4).

Three-dimensional (3D) cell cultures are documented to regain intrinsic properties and to better mimic the *in vivo* situation than cells cultured as monolayers (36, 37). Riedl *et*

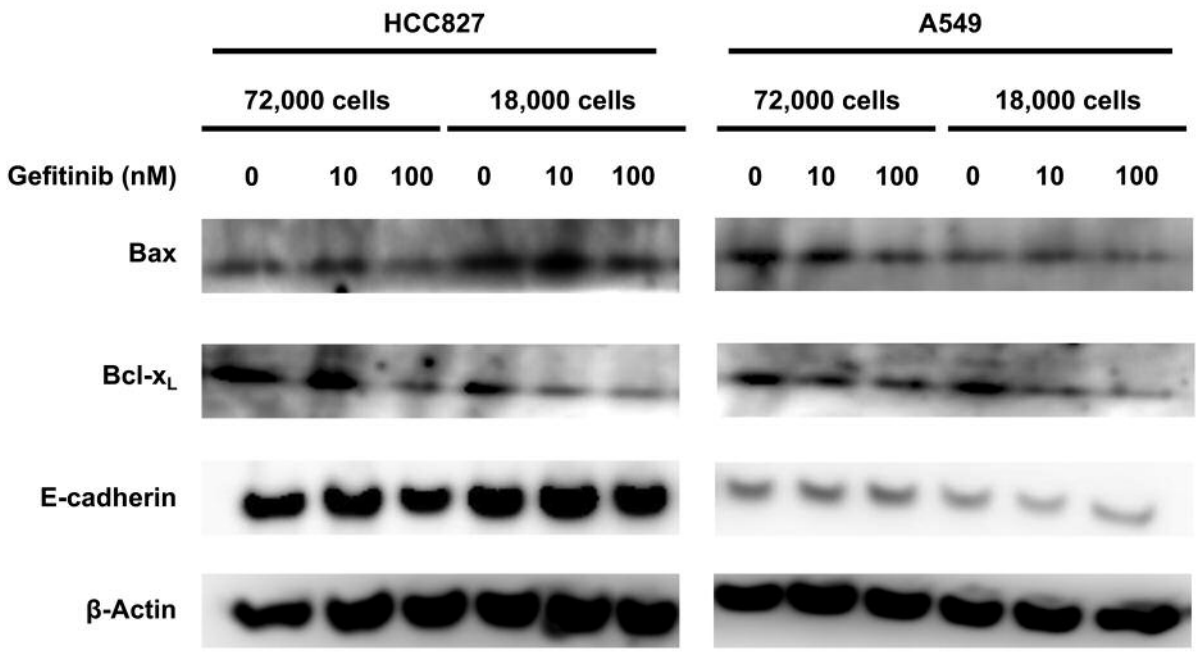

Figure 5. *Effects of cellular numbers and gefitinib treatment in the expression levels of apoptosis-related proteins. Western blot analyses of HCC827 cells or A549 cells (72,000 cells or 18,000 cells originally seeded on microplates as described in the Materials and Methods section) treated with gefitinib (0, 10, or 100 nM) for 72 h at 37˚C, prior to detection of expression levels of Bax, Bcl-xL, E-cadherin, or β-actin using protein specific antibodies.*

al. reported changes of proliferation and metabolic capacity in 3D cell cultures by systematically analyzing spheroids of colon cancer cell lines, showing relative lower activities in the AKT, mammalian target of rapamycin (mTOR) and S6K (RPS6KB1) signaling pathway compared to cells cultured in 2D (36). In our results, HCC827 cell density affected biological activity of STR by gefitinib in HCC827 cells (Figure 1), and cells cultured in the cluster model increased biological activity of STR compared to the dispersed cell culture model (Figure 2). These findings in 3D cell cultures provide fundamental information about effects of gefitinib treatment on mitochondrial functionality in *EGFR* mutants under mimicking the *in vivo* situation.

In the analysis of apoptosis-related protein expression level, expression of Bcl-x_L was increased in a high number of HCC827 cells, and gefitinib treatment (10 nM) kept the Bcl-x_L expression level, suggesting that the high cell number increases the pro-survival efficacy of Bcl-x_L and the gefitinib treatment still keeps it (Figure 5). The increased cell number of HCC827 reduced the Bax expression, and doubled the ratio of Bcl-x_L/Bax (Figure 5), suggesting that a high number of HCC827 cells enhances survival modes. Treatment of gefitinib did not reduce the expression level of E-cadherin, however, we found that high number of HCC827 cells reduced the expression level of E-cadherin, which correlates cell contact and metastasis. Therefore, treatment of a high number of HCC827 cells with gefitinib might possibly reduce apoptotic cell death and enhanced metastasis of HCC827 cells.

In conclusion, we found significant characteristics of gefitinib especially regarding its effects on mitochondrial functionality. Our results indicate that gefitinib may work as a mitochondrial protector against combinational treatment with mitochondria-dependent anti-cancer agents in high-cell-density. Although further studies are needed to elucidate their molecular mechanisms as to these biological phenomena described above, our findings will open avenues for development of novel medical methodologies to improve anti-cancer treatment, and understanding hidden biological and chemical functionality of gefitinib including enhancement of mitochondrial functions found in this research should be highly regarded for future therapy.

Conflicts of Interest

The Authors declare no conflicts of interest.

Acknowledgements

The Authors would like to acknowledge that this work was supported in part by JSPS KAKENHI (JP16H02612 for I.N.). This work was also supported by the Leading University as a Base for Human Resource Development in Nanoscience and Nanotechnology, Osaka Prefecture University. S.S.K. was supported by National Institution

of Health (R21CA178301 and R01CA169259), American Cancer Society (RSG-13-047), and Harvard Stem Cell Institute Blood Program (DP-0110-12-00). The manuscript preparation was assisted by Kayo Hirano (Osaka Prefecture University).

References

1 Berardi R, Santoni M, Morgese F, Ballatore Z, Savini A, Onofri A, Mazzanti P, Pistelli M, Pierantoni C, De Lisa M, Caramanti M, Pagliaretta S, Pellei C and Cascinu S: Novel small molecule EGFR inhibitors as candidate drugs in non-small cell lung cancer. Onco Targets Ther *6*: 563-576, 2013.

2 Segovia-Mendoza M, González-González ME, Barrera D, Díaz L and García-Becerra R: Efficacy and mechanism of action of the tyrosine kinase inhibitors gefitinib, lapatinib and neratinib in the treatment of HER2-positive breast cancer: preclinical and clinical evidence. Am J Cancer Res *5*: 2531-2561, 2015.

3 Segovia-Mendoza M, Díaz L, González-González ME, Martínez-Reza I, García-Quiroz J, Prado-Garcia H, Ibarra-Sánchez MJ, Esparza-López J, Larrea F and García-Becerra R: Calcitriol and its analogues enhance the antiproliferative activity of gefitinib in breast cancer cells. J Steroid Biochem Mol Biol *148*: 122-131, 2015.

4 Watanabe S, Inoue A, Nukiwa T and Kobayashi K: Comparison of Gefitinib *versus* chemotherapy in patients with non-small cell lung cancer with exon 19 deletion. Anticancer Res *35*: 6957-61, 2015.

5 Otsuka T, Mori M, Yano Y, Uchida J, Nishino K, Kaji R, Hata A, Hattori Y, Urata Y, Kaneda T, Tachihara M, Imamura F, Katakami N, Negoro S, Morita S and Yokota S: Effectiveness of Tyrosine kinase inhibitors in Japanese patients with non-small cell lung cancer harboring minor epidermal growth factor receptor mutations: Results from a Multicenter Retrospective Study (HANSHIN Oncology Group 0212). Anticancer Res *35*: 3885-3891, 2015.

6 Umbreit C, Erben P, Faber A, Hofheinz RD, Aderhold C, Weiss C, Hoermann K, Wenzel A and Schultz JD: MMP9, Cyclin D1 and β-Catenin are useful markers of p16-positive squamous cell carcinoma in therapeutic EGFR inhibition *in vitro*. Anticancer Res *35*: 3801-10, 2015.

7 Wang, J, Wang B, Chu H and Yao Y: Intrinsic resistance to EGFR tyrosine kinase inhibitors in advanced non-small-cell lung cancer with activating EGFR mutations. Onco Targets Ther *9*: 3711-3726, 2016.

8 Ni J and Zhang L: Evaluation of three small molecular drugs for targeted therapy to treat non-small cell lung cancer. Chin Med J *129*: 332-340, 2016.

9 Sainsbury JRC, Farndon JR, Harris AL and Sherbet GV: Epidermal growth factor receptors on human breast cancers. Br J Surg *72*: 186-188, 1985.

10 Ferrero JM, Ramaioli A, Largillier R, Formento JL, Francoual M, Ettore F, Namer M and Milano G: Epidermal growth factor receptor expression in 780 breast cancer patients: a reappraisal of the prognostic value based on an eight-year median follow-up. Ann Oncol *12*: 841-846, 2001.

11 Shigematsu, H and Gazdar AF: Somatic mutations of epidermal growth factor receptor signaling pathway in lung cancers. Int J Cancer *118*: 257-262, 2006.

12 Kobayashi S, Ji H, Yuza Y, Meyerson M, Wong KK, Tenen DG and Halmos B: An alternative inhibitor overcomes resistance caused by a mutation of the epidermal growth factor receptor. Cancer Res *65*: 7096-7101, 2005.

13 Kobayashi S, Boggon TJ, Dayaram T, Jänne PA, Kocher O, Meyerson M, Johnson BE, Eck MJ, Tenen DG and Halmos B: EGFR mutation and resistance of non-small-cell lung cancer to gefitinib. N Engl J Med *352*: 786-792, 2005.

14 Moulder SL, Yakes FM, Muthuswamy SK, Bianco R, Simpson JF and Arteaga CL: Epidermal growth factor receptor (HER1) tyrosine kinase inhibitor ZD1839 (Iressa) inhibits HER2/neu (erbB2)-overexpressing breast cancer cells *in vitro* and *in vivo*. Cancer Res *61*: 8887-8895, 2001.

15 Anido J, Matar P, Albanell J, Guzmán M, Rojo F, Arribas J, Averbuch S and Baselga J: ZD1839, a specific epidermal growth factor receptor (EGFR) tyrosine kinase inhibitor, induces the formation of inactive EGFR/HER2 and EGFR/HER3 heterodimers and prevents heregulin signaling in HER2-overexpressing breast cancer cells. Clin Cancer Res *9*: 1274-1283, 2003.

16 Campiglio M, Locatelli A, Olgiati C, Normanno N, Somenzi G, Viganò L, Fumagalli M, Ménard S and Gianni L: Inhibition of proliferation and induction of apoptosis in breast cancer cells by the epidermal growth factor receptor (EGFR) tyrosine kinase inhibitor ZD1839 ('Iressa') is independent of EGFR expression level. J Cell Physiol *198*: 259-268, 2004.

17 Moasser MM, Basso A, Averbuch SD and Rosen N: The tyrosine kinase inhibitor ZD1839 ("Iressa") inhibits HER2-driven signaling and suppresses the growth of HER2-overexpressing tumor cells. Cancer Res *61*: 7184-7188, 2001.

18 Krol J, Francis RE, Albergaria A, Sunters A, Polychronis A, Coombes RC and Lam EW: The transcription factor FOXO3a is a crucial cellular target of gefitinib (Iressa) in breast cancer cells. Mol Cancer Ther *6*: 3169-3179, 2007.

19 Costa DB, Halmos B, Kumar A, Schumer ST, Huberman MS, Boggon TJ, Tenen DG and Kobayashi S: BIM mediates EGFR tyrosine kinase inhibitor-induced apoptosis in lung cancers with oncogenic EGFR mutations. PLoS Med *4*: 1669-1679, 2007.

20 Bhosle J, Kiakos K, Porter AC, Wu J, Makris A, Hartley JA and Hochhauser D: Treatment with gefitinib or lapatinib induces drug resistance through downregulation of topoisomerase IIalpha expression. Mol Cancer Ther *12*: 2897-2908, 2013.

21 Slater TF, Sawyer B and Straeuli U: Studies on succinate-tetrazolium reductase systems. III. Points of coupling of four different tetrazolium salts. Biochim Biophys Acta *77*: 383-393, 1963.

22 Baker MA, Krutskikh A, Curry BJ, Hetherington L and Aitken RJ: Identification of cytochrome-b5 reductase as the enzyme responsible for NADH-dependent lucigenin chemiluminescence in human spermatozoa. Biol Reprod *73*: 334-342, 2005.

23 Blacker TS, Chen W, Avezov E, Marsh RJ, Duchen MR, Kaminski CF and Bain AJ: Investigating mitochondrial redox state using NADH and NADPH autofluorescence. Free Radic Biol Med *100*: 53-65, 2016.

24 Smiley ST, Reers M, Mottola-Hartshorn C, Lin M, Chen A, Smith TW, Steele GD Jr. and Chen LB: Intracellular heterogeneity in mitochondrial membrane potentials revealed by a J-aggregate-forming lipophilic cation JC-1. Proc Natl Acad Sci USA *88*: 3671-3675, 1991.

25 Momparler RL, Karon M, Siegel SE and Avila F: Effect of adriamycin on DNA, RNA, and protein synthesis in cell-free systems and intact cells. Cancer Res *36*: 2891-2895, 1976.

26 Frederick CA, Williams LD, Ughetto G, van der Marel GA, van Boom JH, Rich A and Wang AH: Structural comparison of anticancer drug-DNA complexes: adriamycin and daunomycin. Biochemistry *29*: 2538-2549, 1990.

27 Gewirtz DA: A critical evaluation of the mechanisms of action proposed for theantitumor effects of the anthracycline antibiotics adriamycin and daunorubicin. Biochem Pharmacol *57*: 727-741, 1999.

28 Thorn CF, Oshiro C, Marsh S, Hernandez-Boussard T, McLeod H, Klein TE and Altman RB: Doxorubicin pathways: pharmacodynamics and adverse effects. Pharmacogenet Genomics *21*: 440-446, 2011.

29 Westphal D, Kluck RM and Dewson G: Building blocks of the apoptotic pore: how Bax and Bak are activated and oligomerize during apoptosis. Cell Death Differ *21*: 196-205, 2014.

30 Tsujimoto Y and Shimizu S: VDAC regulation by the Bcl-2 family of proteins. Cell Death Differ *7*: 1174-1181, 2000.

31 Delbridge AR and Strasser A: The BCL-2 protein family, BH3-mimetics and cancer therapy. Cell Death Differ *22*: 1071-1080, 2015.

32 van Roy F and Berx G: The cell-cell adhesion molecule E-cadherin. Cell Mol Life Sci *65*: 3756-3788, 2008.

33 Xia S and Laterra J: Hepatocyte growth factor increases mitochondrial mass in glioblastoma cells. Biochem Biophys Res Commun *345*: 1358-1364, 2006.

34 Tan DX, Manchester LC, Qin L and Reiter RJ: Melatonin: A Mitochondrial Targeting molecule involving mitochondrial protection and dynamics. Int J Mol Sci *17*: E2124, 2016.

35 Mott JL, Zhang D, Freeman JC, Mikolajczak P, Chang SW and Zassenhaus HP: Cardiac disease due to random mitochondrial DNA mutations is prevented by cyclosporin A. Biochem Biophys Res Commun *319*: 1210-1215, 2004.

36 Riedl A, Schlederer M, Pudelko K, Stadler M, Walter S, Unterleuthner D, Unger C, Kramer N, Hengstschläger M, Kenner L, Pfeiffer D, Krupitza G and Dolznig H: Comparison of cancer cells in 2D *vs*. 3D culture reveals differences in AKT-mTOR-S6K signaling and drug responses. J Cell Sci *130*: 203-218, 2017.

37 Dolznig H, Rupp C, Puri C, Haslinger C, Schweifer N, Wieser E, Kerjaschki D and Garin-Chesa P: Modeling colon adenocarcinomas *in vitro* a 3D co-culture system induces cancer-relevant pathways upon tumor cell and stromal fibroblast interaction. Am J Pathol *179*: 487-501, 2011.

Received June 27, 2017
Revised July 9, 2017
Accepted July 10, 2017